Simulations of Corrosion and Passivation Phenomena: Diffusion Feedback on the Corrosion Rate

A. Taleb,[†] A. Chaussé,[†] M. Dymitrowska,[†] J. Stafiej,[†,‡] and J. P. Badiali*[,§]

Laboratoire Analyse et Environnement, UMR 8587, Université d'Evry Val d'Essonne, Bd F. Mitterrand, 91025 Evry, France, Institute of Physical Chemistry, Polish Academy of Sciences, ul. Kasprzaka 44/52, 01-224 Warsaw, Poland, and Laboratoire d'Electrochimie et de Chimie Analytique, ENSCP et Université P. et M. Curie, UMR 7575, 4. Place Jussieu, 75005 Paris, France

Received: May 19, 2003; In Final Form: October 21, 2003

We use a simple cellular automata type model to describe the role of diffusion and reaction processes in the formation of films on a surface. At a mesoscopic scale we select three main processes present during the formation of real interfaces: the corrosion of the metal at the corrosion front, the redistribution of the intermediate corrosion products across the layer already formed, and their precipitation at the growth front. The redistribution of the intermediate corrosion products is modeled as a diffusion of a chemical species. As the concentration of this species at the corrosion front can be large, we have to consider their interactions which is the new aspect of this model. As a result we have a feedback effect on the evolution and structure of the corrosion front. We show that the initial corrosion rate is progressively decreased to the corrosion rate limited by the diffusion process. The corrosion front becomes flat and loses the fractal character present in the corresponding model without the feedback effect. The flattening of the corrosion front increases the protective effect and slows down the corrosion rate. Thus, the overall passivation results from a combination of these two effects. The simple exclusion principle adopted in the model leads to highly nonlinear couplings between the processes involved. The nonlinear dynamics is seen in the time dependence of the diffusing species profile across the layer.

1. Introduction

The processes of growth have given rise to many theoretical investigations during the last fifteen years (see, for instance, ref 1). A large part of these works are based on numerical simulations. The Eden model[2] and the so-called diffusion-limited aggregation (DLA) model[3] represent two basic starting points from which a theoretical description can be elaborated. In domains of practical importance, the growth of a film surface results from a large number of processes, for instance, chemical and electrochemical reactions, diffusion, migration, and heat dissipation. We have also to consider intricate couplings between these processes. The formation of films on a surface is associated with corrosion, and their growth can be partially limited by passivation processes. A theoretical investigation of films formed in such conditions requires an extension of the basic models of growth.

A brute force approach should consist of taking into account all the phenomena that appear in real systems. This is a quite impossible task, and in fact, all the models are based on a given choice of processes that are assumed to be relevant for the time scale or the length scale under consideration. In terms of a continuous description these models lead to solving a set of coupled nonlinear differential equations. At least one part of them are known as *reaction−diffusion equations*. They require a careful treatment as they may exhibit a variety of complex behaviors such as the existence of a multiplicity of states, the presence of oscillatory states, pattern formation, and chaotic evolution.[4,5] The combination of simple processes involving diffusion and reactions represents a typical example of what is called a *complex system*.[6] There, the complexity does not result from the existence of a huge number of processes but from the fact that simple processes may lead to unexpected or unpredictable behaviors. Because diffusion and reaction phenomena are present in the formation of any layer, it is worthwhile to focus on them and elucidate their role. For this reason we do not consider any details of the other mechanisms that may exist at a microscopic level. In other words we perform a description at a mesoscopic scale.

Our main goal is to describe the gross features, which appear in the formation of layers on a surface in the presence of corrosion, diffusion, and precipitation at the growth front. In what follows we focus on the evolution of the corrosion front and a description of its morphology by its roughness and its fractal character. Having in mind this goal, we introduce cellular automata models that have been already extensively used to describe reactive and diffusive systems.[7]

Hereafter, our starting point is the Eden model from which several variants have been already proposed in order to describe electrochemical interfaces. In ref 8 a poisoning effect has been introduced, and it has been shown that a phase transition associated with a percolation process can be observed. In addition, a self-critical behavior appears if a poison produced during the reaction diffuses into the solvent.[9] Recently, the authors have shown that the diffusion of species from the

[†] Université d'Evry Val d'Essonne.
[‡] Polish Academy of Sciences.
[§] ENSCP et Université P. et M. Curie.

10.1021/jp035377g CCC: $27.50
Published on Web 12/24/2003

corrosion front to the growth front changes the physics of the Eden model for the growth front.[10] A smoothing in the roughness of this front is observed, in contrast with the predictions of the Eden model for which the roughness increases as the one-third power of the mean position of the growth front.[1] In the model presented in ref 10, the formation of the layer does not basically change the properties of the corrosion front, which still pertains to the universality class of the Eden model. Moreover, the corrosion rate remains constant during the growth. In this paper we improve this model in order to create a feedback effect of the layer formation on the corrosion rate and to analyze the structure of the corrosion front in such conditions. As we shall see, this feedback effect leads to an effective passivation of the corroding surface. To the best of our knowledge, this is the first example of mesoscopic model describing such phenomena. The paper is organized as follows. In Section 2 we describe a cellular automata model on a two-dimensional lattice. We define the rules for the occupancy of sites and the rules of transformations of these sites to mimic the chemical reaction and diffusion process. To have a complete view of the role of the diffusion on the structure of the corrosion front, in Section 3 we discuss some results for models in which the diffusion is infinitely rapid and for a model in which there is diffusion but no feedback effect. In Section 4 we analyze the complete model focusing on the evolution of the corrosion rate, the distribution of diffusing species in the layer, and the roughness of the front. In the last section we present some concluding remarks.

2. The Model

From a physical point of view we want to mimic the following mechanisms. The layer formed allows for a further corrosion of the material covered by it because of its conductivity or permeability to the species of the aggressive environment. One part of the corrosion products fills up the volume of the just-corroded material while the other part is redistributed by diffusion. It diffuses until it reaches the growth front where in the immediate contact with the aggressive environment it produces an insoluble corrosion product, which precipitates thus advancing the layer growth front. In this model we have two reactions: one on the corrosion front and the other on the growth front. They are coupled by the transport of matter between them via the diffusion process. Such mechanisms are involved in the formation of a large number of real interfaces. For instance, in the case of lithium batteries they partially determine the formation of a passive film on the lithium anode.[11] They are present in corrosion processes on metal surfaces covered by conducting oxide layers[12,13] as well as in the formation of a polymeric film on a copper electrode as shown by experiments.[14] Undoubtedly, such mechanisms exist on an unprotected material exposed to the natural environment.

2.1. Occupation and Transformation of Lattice Sites. To describe the mechanisms mentioned above we perform a simulation on a two-dimensional (2-D) lattice. This reduced dimensionality is chosen mostly to save computational time. Certainly, the simulations of a three-dimensional system would produce a richer class of behaviors. However, as we shall see in Section 4, the physics of the main qualitative features that we find in our 2-D system is independent of the dimensionality. On the same footing we expect that the results quantitatively depend on the geometry of the lattice but that any lattice is sufficient for describing the main features in which we are interested. In what follow we choose a square lattice for reasons of convenience.

The lattice sites can be occupied by four different kinds of species: the metal, the corrosion products, the corrosive species, and the diffusing species. These species will be denoted *M*, *L*, *S* and *D*, respectively, and a site occupied temporarily by an *M* species (few atoms), for instance, will be called an *M* site for the sake of simplicity. The cellular automata model prescribes the rules according to which the sites can be transformed and displaced on the lattice.

Two sites are said to be in contact when they are nearest neighbors. At the beginning of the simulations a first line of *M* sites is in contact with a layer of *L* species. Later in the simulation an *M* site in contact with at least one *L* site is called a reactive site for the corrosion or simply a corrosion site; only this kind of *M* site can be transformed. Similarly, an *S* site in contact with at least one *L* site is defined as a growth site.

The corrosion product formation involves a volume excess that is due to its stoichiometry, so a given volume of the layer filled up with the corrosion products represented by an *L* site need not be formed from corrosion of the equivalent volume of the metal represented by an *M* site.[10] We take this into account by assuming that a site occupied by the metal contains a number $(\phi + 1)$ of *M* species. The corrosion reaction is formally represented by the following reaction scheme:

$$S + (\phi + 1)M \rightarrow L + (\phi)D \qquad (1)$$

The *D* species arises as an intermediate in the conversion of the *M* species into the corrosion product. Its role is then to redistribute the excess volume arising from ϕM via a diffusion process. Because the concentration of the *D* species can be very high near the corrosion front, we cannot neglect their interactions. In what follows we represent these interactions as a steric interaction assuming that at most one diffusing species can occupy an *L* site. This kind of modeling of the steric interaction is commonly used in the literature[15] and is referred to as the simple exclusion rule. Out of the different possibilities in which reaction 1 can be represented in the lattice model, we select those consistent with the simple exclusion rule. As we will see, the constraints thus imposed can change the dynamic character of the corrosion process.

For a given time step δt we select at random a given number, N_{corr}, of corrosion sites that we attempt to transform. If $\phi = 1$, for each selected corrosion site one *D* species has to be inserted in the layer. Then we adopt the following rule. The selected corrosion site is transformed to a layer site and the *D* species is placed in it. At the same time step the *D* species starts executing its random walk in the following way. From among the four nearest neighbors of the transformed site one is selected at random, and if it is a type *L* site, the *D* species is moved there and the transformed site becomes an *L* site. Otherwise, it remains a *D* site. Each attempt to corrode is successful as we can always place the *D* species at the newly created layer site without breaking the simple exclusion rule. Thus, N_{corr} reactive sites are transformed at a time step. If $\phi = 2$, we have to attempt insertion of two new *D* species. One of the nearest neighbors of the site to be corroded is selected at random. If it is a free layer site both sites are converted to *D* sites. In the other case we attempt the random selection for the remaining three and then two nearest neighbor sites. If it turns out with the last one that none of the nearest neighbors is a free layer site, we have decided to adopt the rule that the corrosion is impossible. This seems to us the simplest and most physical of a handful of the possibilities one can consider here to remain consistent with the exclusion rule. Thus, in the case of $\phi = 2$, the outcome of

an attempt to perform reaction 1 is not a priori certain and depends on the situation in the immediate vicinity of the site selected for corrosion. We have created a feedback effect of the layer in formation on the reaction rate. In this simple case we mimic a limitation of the corrosion rate by a concentration overpotential well-known in electrochemistry.[16]

2.2. Diffusion Process. We assume that the *D* species created at the corrosion front perform a random walk on the *L* sites already created. A random walk mimics a self-diffusion process.[17] Note that in our case these walks take place in a nonhomogeneous system. Moreover, a steric interaction between diffusing species is introduced. The model of steric hindrance is similar to that described above. During each time interval δt all walkers attempt to execute one step. Among the four nearest neighbors of a given walker, one is selected at random. If this nearest neighbor is a metal site, no move is made. If the selected nearest neighbor is an *L* site free of *D* species, then the walker is moved to it. The walker stays at its initial position when the selected nearest neighbor is already occupied by a *D* species. If the nearest neighbor is a solvent site, the walker is moved to it and it is immediately converted into an *L* site. This process is represented by our second formal reaction:

$$D + S \rightarrow L \tag{2}$$

Thus, created at the corrosion front, a walker performs a random walk across the layer avoiding other walkers and finishes its existence by entering the solvent where it turns into a layer site. In the practical simulations the list of walkers is permuted randomly at each time step to avoid spurious correlations with the initial setting of the list.

In summary, the model described above is quite simple and contains explicitly only two parameters. One, ϕ, takes into account the excess volume of the layer compared to the corroded volume. Changing ϕ is equivalent to changing the chemical nature of the materials involved in the process. The other parameter, N_{corr}, has a dynamical origin, and it is unavoidable in any process in which there is a reaction−diffusion coupling. N_{corr} is the number of sites that we attempt to corrode in a unit of time diffusion steps performed between two corrosion steps. Implicitly, we assume that the flux of the aggressive species from the environment is so adjusted as to keep constant the intrinsic corrosion rate, that is, the number of attempts to corrode. Note that the model also contains some implicit parameters as those related to the occupancy rules. They have been chosen in order to have processes that are as simple as possible. There is no problem for instance in changing the number of *D* entities that can coexist at the same position, and for this simplest model we can imagine a lot of variants. In comparison with real interfaces our model is extremely crude. Only one species is diffusing, there is no electric effect, and so forth. However, it already contains a lot of physical content as is shown hereafter.

3. Results in Absence of Feedback Effect

Almost all results presented in this paper have been obtained using a simulation box in which there are $N_x = 2000$ units (columns) in the *x* direction and $N_y = 1000$ units (lines) in the *y* direction. Each site, (i, j), is referred by its column *i* and its line *j*. At time $t = 0$, the sites up to line $j = 499$ are filled up with *M* sites. The sites corresponding to $j = 499$ are our initial corrosion sites. Line $j = 500$ is formed of the layer sites containing walkers. From line $j = 501$ and above, the other half of the box is filled up with the solution sites. Periodic boundary conditions are applied in the *x* direction. The lattice spacing is considered as the unit of length; we take $\delta t = 1$, and therefore, the number of diffusion steps, N_t, gives the time during which the system is investigated.

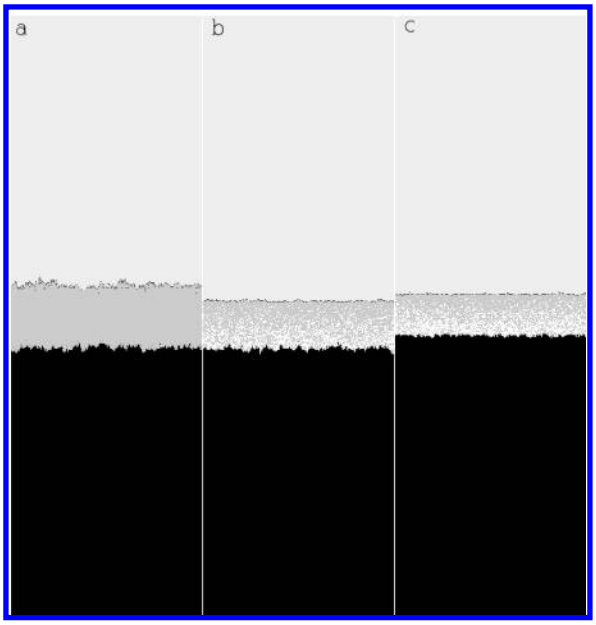

Figure 1. Snapshots taken at the $N_t = 10\,000$ time step for (a) the double-Eden model with $N_{corr} = 10$ and $\phi = 1$, (b) the Eden model for corrosion and the diffusion model for growth with $N_{corr} = 10$ and $\phi = 1$, and (c) the modified model for corrosion and diffusion with $N_{corr} = 10$ and $\phi = 2$.

To illustrate the role of diffusion, we first start with a model in which diffusion does not play any role.

3.1. Double-Eden Model. We consider a simple extension of the Eden model[2] in which the algorithm is reduced to the following steps. We choose at random a corrosion site and transform it into an *L* site while ϕ entities of *M* are placed at random at the positions of growth sites and converted immediately to the *L* sites. With our definition of the reactive sites the algorithm for the growth and the corrosion are the same, and they are identical to the one of the Eden model. In this double-Eden model there is one dynamic process related to the corrosion rate; in comparison to it the diffusion process is assumed to be infinitely rapid. There is no explicit time scale in these simulations. Nevertheless, we can introduce N_{corr} in a purely formal manner, as its main interest is to give us a way to compare the growth and the corrosion in the absence or presence of diffusion.

The results of simulation are presented in Figures 1a and 2a for $\phi = 1$ and $N_{corr} = 10$. They are obtained for the number of time steps, N_t, of 10^4 and 9×10^4, respectively. The layer (middle part of the snapshot, in gray) is located between a black and a white region that represents the metal and the external environment, respectively. The mean position of the growth and corrosion fronts are defined according to

$$\langle h_{growth}(N_t)\rangle = \frac{1}{N_x}\sum_{i=1,N_x} h_{growth}(i) \quad \text{and}$$

$$\langle h_{corr}(N_t)\rangle = \frac{1}{N_x}\sum_{i=1,N_x} h_{corr}(i) \tag{3}$$

in which $h_{growth}(i)$ and $h_{corr}(i)$ are, respectively, for the column *i* the highest value of *j* for which there is an *L* site and a

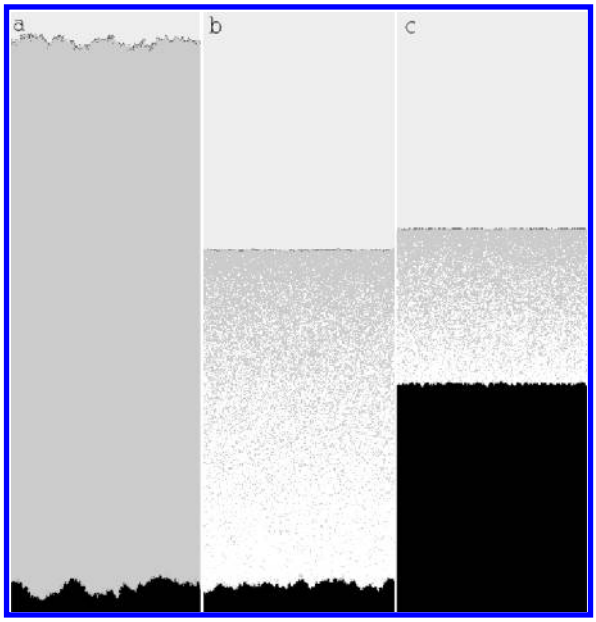

Figure 2. Same snapshots as in Figure 1 taken at the $N_t = 90\,000$ time step.

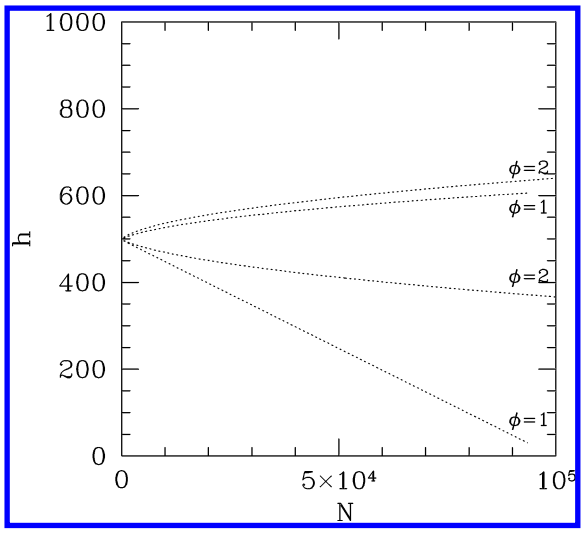

Figure 3. Comparison of the front evolutions in terms of the average positions of the fronts of growth (the two upper curves) and corrosion (two lower curves) and for the two cases of $N_{corr} = 10$, $\phi = 2$ and $N_{corr} = 10$, $\phi = 1$.

corrosion site. The simulation results (Figure 3) verify the linear relations:

$$\langle h_{corr}(N_t)\rangle = h(0) - \frac{N_t N_{corr}}{N_x} \quad \text{and}$$

$$\langle h_{growth}(N_t)\rangle = h(0) + \phi\frac{N_t N_{corr}}{N_x} \quad (4)$$

in which $h(0)$ is the value of j corresponding to the position of the plane separating the metal from the solution at the initial time. To describe the evolution of the corrosion front we introduce a corrosion rate $k(N_t)$ defined according to

$$k(N_t) = \frac{d}{dN_t}[h(0) - \langle h_{corr}(N_t)\rangle] = \frac{d}{dN_t}\Delta h_{corr}(N_t) \quad (5)$$

Here, the corrosion rate is constant and we have $k(N_t) = N_{corr}/N_x$. This represents the number of corroded sites counted per unit of the initial area, N_x, and per unit of time. Although the random choice of the reactive sites does not affect the evolution of $\langle h_{growth}(N_t)\rangle$ and $\langle h_{corr}(N_t)\rangle$, it determines the roughness of the fronts defined according to

$$\sigma_{growth}(N_t) = \left[\frac{1}{N_x}\sum_{i=1,N_x}(h_{growth}(i) - \langle h_{growth}(N_t)\rangle)^2\right]^{1/2} \quad (6)$$

and

$$\sigma_{corr}(N_t) = \left[\frac{1}{N_x}\sum_{i=1,N_x}(h_{corr}(i) - \langle h_{corr}(N_t)\rangle)^2\right]^{1/2} \quad (7)$$

for which we observe the scaling law of the Eden model $\sigma_{growth}(N_t) \propto N_t^{1/3}$ and the same for the corrosion front. In parallel the fronts exhibit a fractal dimension $d_f = 1.5$.[1]

3.2. Growth in the Presence of Diffusion. The snapshots corresponding to $\phi = 1$ are given in Figures 1b and 2b with the others parameters the same as in Figures 1a and 1b. In the layer, the white points correspond to the D species. We can see immediately that the diffusion reduces the roughness of the growth front as already reported in ref 10. *A similar result is obtained experimentally with the anodization of copper in thiourea containing acid solution.*[18] The mean positions of the fronts are given in Figure 3. The properties of the corrosion front are not modified by the diffusion, and in particular, the corrosion rate defined in (5) is unchanged. In contrast the growth front now exhibits a nonlinear behavior. For the largest values of N_t we observe $[\langle h_{growth}(N_t)\rangle - h(0)] \propto (N_t)^{\alpha}$ where α is very close to 0.5 as expected for growth processes determined by diffusion.[19]

4. Corrosion in the Presence of Feedback Effect: Passivation Phenomena

For $\phi = 2$ the growth front exhibits the same properties as in the case of $\phi = 1$; therefore, in this section we essentially focus on the modification of the corrosion front. The snapshots obtained for $\phi = 2$ are shown in Figures 1c and 2c. The comparison of Figures 2b and 2c corresponding to the same $N_t = 9 \times 10^4$, that is, to the same number of corrosion steps, shows that the feedback effect has two main consequences: the thickness of the layer is reduced and a smoothing of the corrosion front is observed. These two aspects characterize the passivation properties of the layer. In what follows these latter aspects will be investigated more quantitatively.

4.1. Evolution of the Corrosion Front. In Figure 3 we can see that the initial corrosion rate $k(N_t)$ corresponding to the limit $N_t \to 0$ is identical to that of the corresponding case for $\phi = 1$ as expected. However, with the increasing number of the simulation time steps we observe that $k(N_t)$ defined according to (5) decreases. We can interpret this result by saying that N_{corr} is now replaced by an effective quantity $N_{corr}(N_t)$ being a decreasing function of N_t.

In the case of $\phi = 2$, the value of $\Delta h_{corr}(N_t) = 125$ is attained at the simulation time $N_t = 10^5$, whereas in the case of $\phi = 1$ when the feedback effect is absent the same value is already obtained at $N_t = 2 \times 10^4$. The corrosion rate is reduced by approximately 1 order of magnitude. For the case of $\phi = 2$, we have continued the simulation up to $N_t = 4.8 \times 10^5$ time steps when $\Delta h_{corr}(N_t) = 310$, and it is approximately 8 times smaller than the value extrapolated for the case of $\phi = 1$. Thus, the doubling of the number of D species created per corrosion event cannot compensate for the reduction of the corrosion rate, and the thickness of the layer is much larger in the case of $\phi = 1$ than in the case of $\phi = 2$.

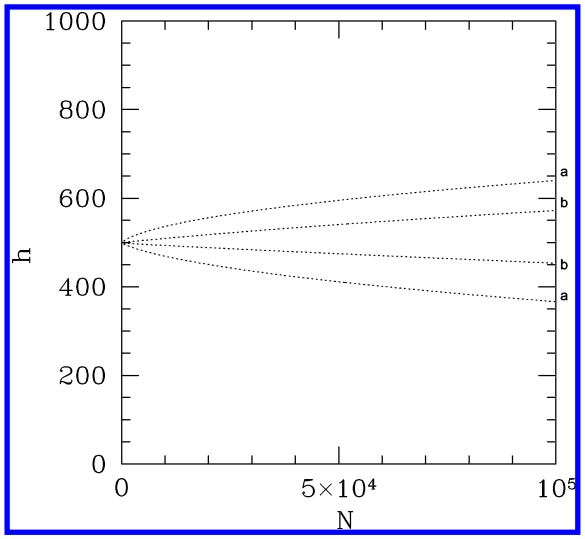

Figure 4. Comparison of the front evolutions as in Figure 3 for $\phi = 2$ and (a) $N_{corr} = 10$, (b) $N_{corr} = 1$.

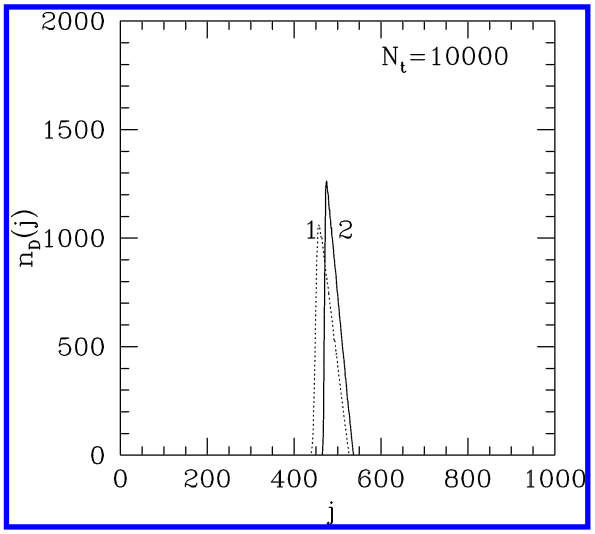

Figure 5. Distribution of walkers at the simulation time $N_t = 10\,000$ for the cases of $\phi = 2$ (solid line) and $\phi = 1$ (dotted line), $N_{corr} = 10$.

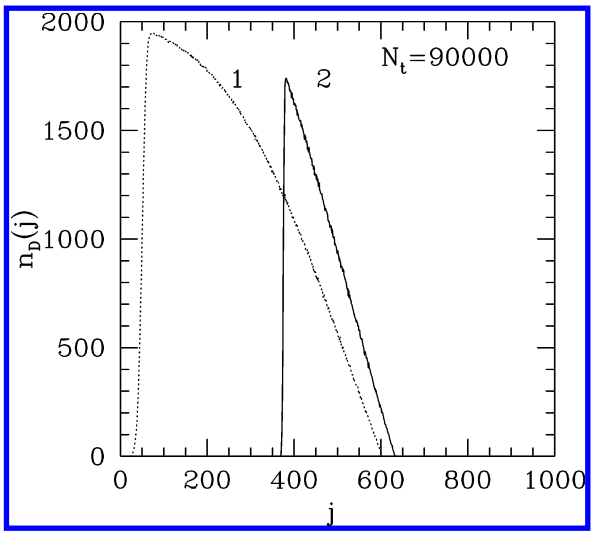

Figure 6. Distribution of walkers at the simulation time $N_t = 900\,000$ for the cases of $\phi = 2$ (solid line) and $\phi = 1$ (dotted line), $N_{corr} = 10$.

Except for times $N_t \rightarrow 0$, the corrosion front exhibits a parabolic evolution. As seen in Figure 3, for the largest values of N_t we have $\Delta h_{corr}(N_t) \propto (N_t)^{\alpha}$ where α is 0.58, and longer simulations show a very slow evolution of α toward 0.5, *which is the value obtained by the experiments in a similar situation*.[18] Figure 3 shows the crossover between two regimes. At short times, $N_t \rightarrow 0$, the corrosion front is not covered by *D* species and each attempt to corrode a site is successful as in the case of $\phi = 1$. After a given number of corrosion steps the corrosion front is both covered by *D* species that block the corrosion and, on average, $N_{corr}(N_t)$ becomes smaller than N_{corr}. However, the coverage of reactive sites by blocking *D* species may change because these *D* species may diffuse. This diffusion can be thought of as being due to other species moving more freely than the *D* species itself. We have in mind holes, which are free layer sites dispersed between the sites occupied primarily by *D* species when the concentration of *D* species is high. A hole can move as a result of swapping with the neighboring *D* species when they happen to step into it. At a distance away from the corrosion front the holes start penetrating the layer of *D* sites blocking the front. In this regime the corrosion rate or $N_{corr}(N_t)$ is determined partially by the initial corrosion rate and by the motion of holes in the vicinity of the corrosion front. In the asymptotic regime in which almost all of the reactive sites are covered by *D* species, the corrosion rate is only determined by the diffusion of holes and a square root dependence in time is expected. As we shall see below (Figure 6), for $N_t = 10^5$ we are not yet in the asymptotic regime, and therefore, the coefficient $\alpha = 0.58$ corresponding to that inFigure 3 describes a crossover situation.

4.2. Role of the Initial Corrosion Rate: Nonlinearity. The processes that we mimic are nonlinear as we can see in Figure 4 where we compare the results obtained with two different initial corrosion rates, that is, for two different values of N_{corr}. A linear behavior should suggest that the value of $\Delta h_{corr}(N_t)$ obtained for $N_{corr} = 1$ and $N_t = 10^5$ (curve a in Figure 4) should be the same as the one obtained with $N_{corr} = 10$ and $N_t = 10^4$ (curve b in Figure 4). This is clearly not the case; the value obtained for $N_{corr} = 10$ is approximately one-half of the value resulting from a linear prediction. Because one-half of the predicted corrosion acts have been effectively performed but 10 walkers are injected into each effective corrosion, we might expect that the total thickness of the layer should be larger when $N_{corr} = 10$ than in the case of $N_{corr} = 1$. The simulations are not in agreement with these predictions. Therefore, it is difficult to predict in a quantitative way the effect of the initial corrosion rate on the behavior of the system in the crossover regime. The intricate coupling between the processes can be illustrated by investigating the distribution of walkers in the layer as a function of N_t.

4.3. Distribution of Walkers. The walker distribution $n_D(j)$ along the direction perpendicular to the initial layer plane is obtained by counting for each line *j* of the square lattice the total number of walkers on this line. In Figures 5 and 6 we compare $n_D(j)$, for $\phi = 1$ and $\phi = 2$, at two different times corresponding to $N_t = 10^4$ and 9×10^4, respectively. In both cases we take $N_{corr} = 10$. The walker distributions given in Figure 5 correspond to the snapshots presented in parts b and c of Figure 1. The two $n_D(j)$ have the same form; however, for $\phi = 1$ the faster advancement of the corrosion front and the slower advancement of the growth compared to the case of $\phi = 2$ are already clearly visible. The part of the distribution located below the maximum corresponds to the corrosion front, and we see that $n_D(j)$ tends to be larger when ϕ is increased. These qualitative features are even more pronounced at the later stage (Figure 6) except for the fact that now the maximum value of the walker distribution is higher for $\phi = 1$ and quite close to the saturation value $N_x = 2000$ in which all possible sites

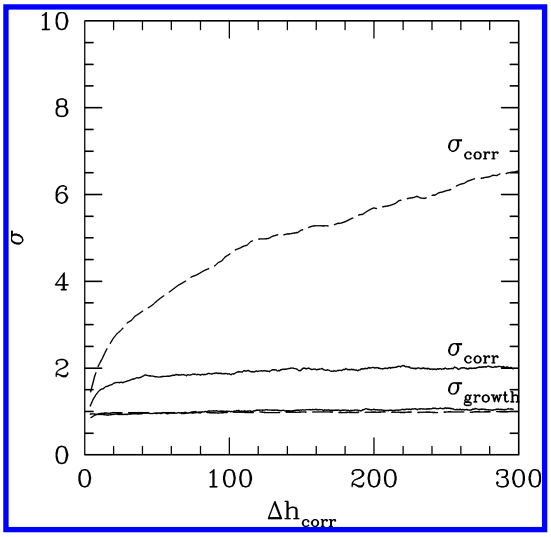

Figure 7. Front roughness measured by the square root of the mean square deviation for $N_{corr} = 10$, $\phi = 1$ (dotted lines) and $\phi = 2$ (solid lines) for the growth fronts (lower curves) and corrosion fronts (upper curves) as a function of the amount of material corroded Δh_{corr}.

existing in a line are occupied by walkers. This limited value for the density of *D* species on each line is a consequence of our model for the steric interaction, and we can conclude that the steric interactions originate from a nonuniform gradient for $n_D(j)$ in the layer. The maximum value for $\phi = 2$ is somewhat lower; approximately 90% of the reactive sites are blocked. This also shows that in the case of Figure 3 we do not reach saturation.

The area under the distributions $n_D(j)$ shows that the total number of walkers is strongly reduced by the feedback effect although the number of *D* species inserted is 2 times more than in the case of $\phi = 1$. The total number of walkers is reduced when we go from $\phi = 1$ to $\phi = 2$; however, the gradient of the walker concentration is higher in the latter case. Accordingly, the diffusion process is more efficient in the case of $\phi = 2$. Thus, we see that the structure of the layer results from a competition between the blocking of the corrosion front and an increase in the diffusion efficiency. The stronger the blocking is, the smaller the number of diffusing species is and accordingly the larger the efficiency of the diffusion is that tends to move away the blocking *D* species. This illustrates how the simple algorithm that we use leads to a strong competition between processes and finally to results that are difficult to predict.

4.4. Roughness of the Front. The smoothing of the corrosion front *predicted by our model* and already seen in Figures 1c and 2c shows that we are no longer in the universality class of the Eden model. *Haseeb et al. show the same consequence of the diffusion on the roughness of the surface in a study on the anodization of copper in thiourea*.[18] In Figure 7 we see that $\sigma_{corr}(N_t)$ defined according to (7) is independent of the position of the corrosion front and then time independent. The mechanism stabilizing the roughness of the front can be described as follows. As we have seen in subsection 4.1 for the long-time behavior, the evolution of the front is determined by the concentration of holes in its vicinity. Now, more accurately we can say that the structure of the corrosion front depends on the gradient of concentration for the holes. Mainly, the holes are created in a region where the *D* species move more freely, and then the probability of arriving at the corrosion front is nonuniform. This is illustrated in Figure 8. For a hole the probability of arriving at the point A is larger than the probability of reaching point B. Thereforesite A is more readily corroded

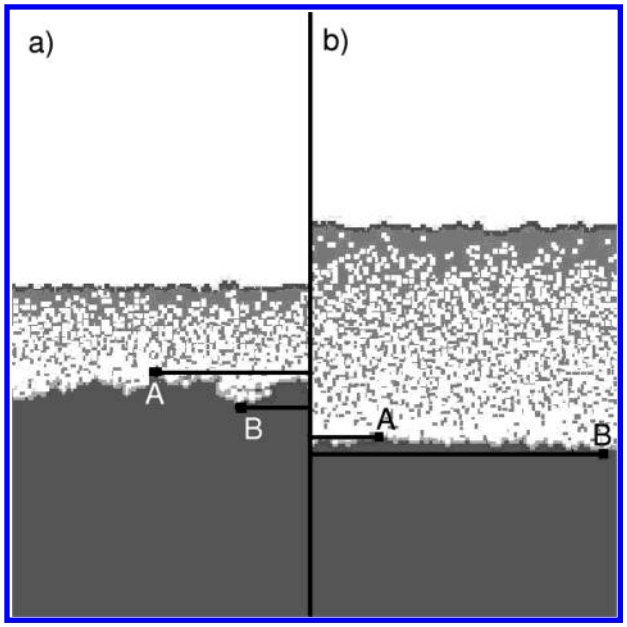

Figure 8. Schematic presentation of the feedback effect on the corrosion front. (a) Rough front of Eden type obtained after 430 simulation steps with parameters $N_{corr} = 10$ and $\phi = 1$ (no feedback) and the simulation box 200×200. (b) The front after 4000 time steps when the initial configuration was that of (a) but the parameter ϕ was set to 2 (feedback effect switched on). Points A mark the uppermost and points B the lowermost positions of the corrosion front.

than site B. As a result during the front evolution the front tends to move faster at the position of site A than at that of the lower site B until the difference in the probability of corrosion between sites becomes insignificant. From the simulations it appears that this happens when the distance between site A and site B is about two lattice spacings. Of course in this case the front is no longer fractal, and no significant value for the fractal dimension can be obtained from the simulation results.

5. Concluding Remarks

In this paper we have investigated phenomena which determine, at least partially, the formation of films at real interfaces (passivation of a lithium anode, formation of polymeric film, material−environment interface). In the simple model that has been developed, the dynamical phenomena of diffusion and reaction are influenced by steric interactions. We have to consider these interactions because the concentration of various species involved in the mechanisms of corrosion can be very high near the corrosion front. The steric effects change the corrosion rate and the efficiency of the diffusion, and they introduce a sophisticated coupling between these two processes. Because of this we have seen that we may generate a rich class of behaviors, and in general, the relations between the processes appear to be nonlinear.

The model gives a simple description of well-known phenomena in electrochemistry. The blocking of corrosion sites by the *D* species can be associated with the concentration overpotential, and the feedback effect of the layer in formation on the corrosion rate is similar to a passivation effect.

The main results can be summarized as follows. For a system in which the initial corrosion rate is high compared to the diffusion rate, the corrosion products can stay on the corrosion front and block the corrosion mechanism. However, the diffusion is not totally impeached because the holes may arrive in the vicinity of the corrosion front. Thus the long-time behavior of the corrosion rate is no longer determined by the initial corrosion

rate but by the diffusion process. The simulations show the transition between these two regimes. The diffusion of holes produces, as a consequence, flattening of the corrosion front. The long-time structure of the corrosion front results from a compromise. On the one hand a high initial corrosion rate produces a blocking of the corrosion sites, decreases the corrosion rate, and therefore reduces the number of the diffusing species inserted into the layer. On the other hand the decrease of the rate of production of the *D* species gives a better opportunity for the holes to arrive and sustain the corrosion rate.

The mechanisms that we have observed in our 2-D simulations are general enough to extend the conclusions to interfaces in the 3-D geometry of the real world. Thus, more generally from our simulations we learn that the passivation of a surface is a sophisticated process. In addition to an obvious decrease of the corrosion rate, we may also observe a self-protection of the metal associated with a flattening of the corrosion front. Because of this effect, the contact surface between the material and the solution containing aggressive species is limited and moreover the smoothing of the front is not favorable to the initiation of a pitting corrosion.

The richness of behaviors that may result from reaction−diffusion processes has been enhanced here by introducing in a simple way natural steric interactions between the species. Note also that the processes that appear in the simulations are difficult to describe a priori using a set of deterministic partial differential equations. Our description can be extended in several ways. We may consider that the corrosion probability at a given site depends on the local morphology of the front. Preliminary results have been already obtained,[20] and they show the possibility of having a quasi-oscillatory behavior for the corrosion front. Another possible extension consists of considering a partial dissolution of the layer.

References and Notes

(1) Barabasi, A. L.; Stanley, H. E. *Fractal Concepts in Surface Growth*; Cambridge University Press: Cambridge, New York, 1995.

(2) Eden, M. *Proceedings of the Fourth Berkeley Symposium on Mathematical Statistics and Probability*; University of California Press 1: Berkeley, CA, 1961; Vol. 4, p 223.

(3) Somfai, E.; Sander, L. M.; Ball, R. C. *Phys. Rev. Lett.* **1999**, *83*, 5523.

(4) Nicolis, G.; Prigogine, I. *Self-organization in Nonequilibrium Systems*; Wiley-Interscience: New York, 1977.

(5) Baras, F.; Mansour, M. *Adv. Chem. Phys.* **1997**, *100*, 393.

(6) Nicolis, G.; Prigogine, I. In *Exploring Complexity*; Freeman: New York, 1989.

(7) Weimar, J. R.; Boon, J-P. *Phys. Rev. E* **1994**, *49*, 1749.

(8) Lafage, M.; Russier, V.; Badiali, J. P. *J. Electroanal. Chem.* **1998**, *450*, 203.

(9) Nainville, I.; Lemarchand, A.; Badiali, J. P. *Phys. Rev. E* **1996**, *53*, 2537.

(10) Taleb, A.; Stafiej, J.; Chausse, A.; Messina, R.; Badiali, J. P. *J. Electroanal. Chem.* **2001**, *500*, 554.

(11) Aurbach, D.; Ein Ely, Y.; Chusid, O.; Carmeli, Y.; Babai, M. *J. Electrochem. Soc.* **1994**, *141*, 603.

(12) Sarrazin, P.; Galerie, A.; Fouletiere, J. Les Mecanisme de la Corrosion Seche—Une Approche Cinétique; Monographies de Matériologie; EDP Sciences, 2000.

(13) Savoye, S.; Legrand, L.; Sagon, G.; Le Comte, S.; Chaussé, A.; Messina, R.; Toulhoat, P. *Corros. Sci.* **2001**, *43*, 2049.

(14) Bolzàn, A. E.; Haseeb, A. S. M. A.; Schilardi, P. L.; Piatti, R. C. V.; Salvarezza, R. C.; Arvia A. J. *J. Electroanal. Chem.* **2001**, *500*, 533.

(15) Nicolis, C.; Kozak, J. J.; Nicolis, G. *J. Chem. Phys.* **2001**, *115*, 663.

(16) Bard, A. J.; Faulkner, L. B. *Electrochemical Methods: Fundamentals and Applications*; John Wiley and Sons: New York, 1980.

(17) Itzykson, C.; Drouffe, J. *Statistical Field Theory*; Cambridge University Press: Cambridge, U.K., 1989.

(18) Haseeb, A. S. M. A.; Schilardi, P. L.; Bolzan, A. E.; Piatti, R. C. V.; Salvarezza, R. R.; Arvia, A. J. *J. Electroanal. Chem.* **2001**, *500*, 543.

(19) Cabrera, N.; Mott, N. F. *Rep. Prog. Phys.* **1948**, 12, 163.

(20) Saunier, J. Private communication.